

2024

Dual TYK2/JAK1 kinase inhibitor suppresses cytoplasmic dsRNA-induced toxic innate immune response in neurodegenerative mice

<https://hdl.handle.net/2144/51383>

"Downloaded from OpenBU. Boston University's institutional repository."

BOSTON UNIVERSITY

ARAM V. CHOBANIAN & EDWARD AVEDISIAN SCHOOL OF MEDICINE

Thesis

**DUAL TYK2/JAK1 KINASE INHIBITOR SUPPRESSES CYTOPLASMIC
DSRNA-INDUCED TOXIC INNATE IMMUNE RESPONSE IN
NEURODEGENERATIVE MICE**

by

DARIA KOMARNITSKY

B.S., University of Massachusetts Amherst, 2022

Submitted in partial fulfillment of the
requirements for the degree of
Master of Science

2024

© 2024 by
DARIA KOMARNITSKY
All rights reserved.

Approved by

First Reader

Haya Herscovitz, Ph.D.
Assistant Professor, Pharmacology, Physiology & Biophysics

Second Reader

Mark Albers, M.D., Ph.D.
Assistant Professor of Neurology
Harvard Medical School

Third Reader

Alexei Degterev, Ph.D.
Associate Professor of Developmental, Molecular, and
Chemical Biology
Tufts University

**DUAL TYK2/JAK1 KINASE INHIBITOR SUPPRESSES CYTOPLASMIC
DSRNA-INDUCED TOXIC INNATE IMMUNE RESPONSE IN
NEURODEGENERATIVE MICE**

DARIA KOMARNITSKY

ABSTRACT

Neurodegenerative diseases such as Alzheimer's disease (AD), frontotemporal dementia (FTD), and amyotrophic lateral sclerosis (ALS) affect millions of people worldwide. Although there are no cures for these debilitating diseases, new potential treatment plans to help patients are being developed. Recent studies have shown that neuroinflammation is a cause of neurodegeneration, and it is triggered by the presence of cytoplasmic double-stranded RNA (cdsRNA) in the cytoplasm of neurons. This insight is being leveraged translationally to produce drugs that block the type I interferon signaling pathway, the innate immune response triggered by cdsRNA, and neural cell death. In this study we examined whether two compounds, TLL041 and TLL082, which inhibit the activity of TYK2 and JAK1 kinases associated with signaling the type I interferon receptor, can block neuroinflammation and cell death. The effects of TLL041 and TLL082 were evaluated *in vivo* in the Nd1 mouse model of neurodegeneration, compared to the isogenic wildtype BL6 mouse. Two doses of each drug (3.3 mg/kg and 10 mg/kg) were administered for 28 consecutive days via oral gavage and the inflammatory marker expression levels in the olfactory sensory neurons determined by qPCR and IHC antibody

staining. Analysis demonstrated that neuroinflammation in Nd1 mice was significantly reduced ($p < 0.05$). These findings indicate that TYK2 and JAK1 kinases are effective drug targets for neuroinflammation in this model of neurodegenerative disease and may potentially be used to slow the progression of neurodegenerative diseases.

TABLE OF CONTENTS

ABSTRACT.....	iv
TABLE OF CONTENTS.....	vi
LIST OF TABLES.....	vii
LIST OF FIGURES.....	viii
LIST OF ABBREVIATIONS.....	ix
INTRODUCTION.....	1
MATERIALS.....	11
METHODS.....	12
RESULTS.....	27
DISCUSSION.....	38
CONCLUSION.....	47
REFERENCES.....	49
VITA.....	52

LIST OF TABLES

Table 1. Disposition of mice across control and experimental groups.....	11
Table 2. qPCR 96-well Plate Setup.....	23
Table 3. RNA/cDNA Counts and Ratios.....	29
Table 4. RNA/cDNA Counts and Ratios after RNA repurification.....	31
Table 5. Treatment group inflammatory marker expression and p-values.....	32

LIST OF FIGURES

Figure 1. Type I IFN pathway illustration.....	4
Figure 2. Maturation of olfactory sensory neurons.....	7
Figure 3. ReN VM cell study results.....	9
Figure 4. Mouse weights over treatment period.....	28
Figure 5. STAT1 gene expression.....	34
Figure 6. MDA5 gene expression.....	35
Figure 7. IFI44 gene expression.....	36
Figure 8. OASL2 gene expression.....	37

LIST OF ABBREVIATIONS

AD.....	Alzheimer's disease
ALS.....	Amyotrophic lateral sclerosis
cdsRNA.....	Cytoplasmic double-stranded RNA
DSBs.....	Double-strand breaks
dsRNA.....	Double-stranded RNA
ERV.....	Endogenous retroviruses
FTD.....	Frontotemporal dementia
IFN-I.....	Type I interferon
ISGs.....	Interferon stimulated genes
JAK1.....	Janus activated kinase 1
OSN.....	Olfactory sensory neuron
PRRs.....	Pattern recognition receptors
PSP.....	Progressive supranuclear palsy
TYK2.....	Tyrosine kinase 2

INTRODUCTION

Cytoplasmic double-stranded RNA (c dsRNA), most commonly generated through viral replication, is a well-established trigger of innate immunity. The inflammatory response that results from the presence of c dsRNA has previously been modeled by introducing synthetic analogue poly I:C into the brains of mice. Various inflammatory markers were found to be elevated in mice treated with poly I:C in comparison to control mice that didn't receive the treatment (Field et al., 2010). Several neurodegenerative diseases have been linked to c dsRNA. One study found that there were elevated amounts of c dsRNA in the brains of deceased amyotrophic lateral sclerosis (ALS) patients and frontotemporal dementia (FTD) patients carrying the C9ORF72 mutation. This mutation, an intronic hexanucleotide expansion that generates c dsRNA, is a common cause of familial and sporadic ALS/FTD (Rodriguez et al., 2021). Another potential origin of dsRNA in ALS is loss of TDP-43 function (LaRocca et al., 2019).

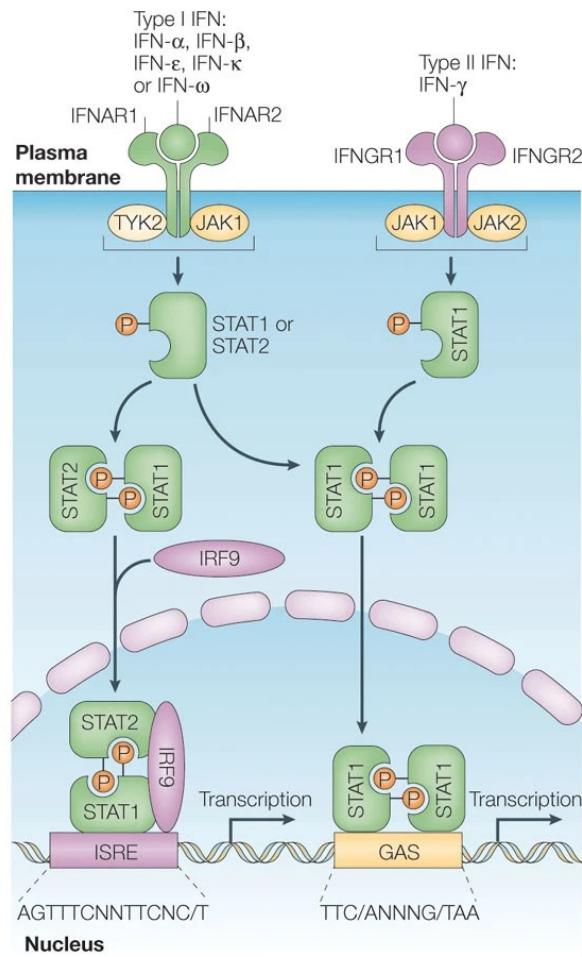
Alzheimer's disease (AD) is a type of tauopathy, meaning aggregates of tau protein are found in the brains of individuals who are affected by the disease. Tau transgenic mice were shown to have elevated levels of a class of retrotransposons called endogenous retroviruses (ERV), indicating that pathogenic tau may be linked to the activation of retrotransposons (Ramirez et al., 2022). Double stranded RNA (dsRNA) can be derived from retrotransposons

when they are activated, and one study found that patients with tauopathies such as AD or progressive supranuclear palsy (PSP) had elevated levels of retrotransposon-derived dsRNA in their astrocytes. This result serves as further evidence that dsRNA plays an important role in the progression of neurodegenerative diseases (Ochoa et al., n.d.). The exact origin of dsRNA in humans is still not fully established, as there are many ways in which it can be generated. Another study showed that there was an accumulation of DNA double-strand breaks (DSBs) in neurons, astrocytes, and oligodendrocytes in the postmortem brains of early AD patients (Dileep et al., 2023). DSBs can cause genomic instability, which if not properly fixed, can result in genetic mutations that could be a potential origin of dsRNA (Domingo-Prim et al., 2020).

Regardless of how dsRNA is generated, it is a well-established driver of neuroinflammation. This was confirmed by a study that examined the effect of introducing dsRNA into the cytoplasm of human neural cells differentiated from human ReN cell VM neuroprogenitors. These are human neural progenitor cells that were transfected with genes containing mutations (APP gene with *Swedish/London* FAD mutations (APPSL) and PSEN1 gene with E9 FAD mutation) associated with familial AD (FAD) to mimic the neurons of patients with neurodegenerative diseases (Kim et al., 2015). Twenty four hours post-transfection with dsRNA, these cells showed elevated expression of several interferon stimulated genes (ISGs) as ISG proteins like MDA5, PKR, and p-

STAT1 were observed, indicating that the presence of dsRNA triggered type 1 interferon (IFN-I) signaling (Rodriguez et al., 2021). Pattern recognition receptors (PRRs) are known to be responsive to dsRNA as a ligand. MDA5 is a type of PRR, and to check its role in the activation of the IFN-I signaling pathway, a knockout of MDA5 was generated in the same study. The removal of MDA5 resulted in a 30% decrease of dsRNA-mediated neuronal death, providing evidence that MDA5 is a PRR involved in dsRNA recognition (Rodriguez et al., 2021). This study showed that failure to recognize dsRNA takes away IFN-I signaling that normally would have occurred if the pattern recognition receptor for dsRNA was present.

The binding of dsRNA to MDA5 ultimately results in the transcription of genes encoding IFN-I (Barrat et al., 2016). IFN-I is released from their cells of origin and are then recognized by type I IFN receptors on the surfaces of human neural cells. These receptors are composed of two subunits, IFNAR1 and IFNAR2. IFNAR1 is associated with a Janus activated kinase (JAK1), while IFNAR2 is associated with a tyrosine kinase 2 (TYK2). The activation of these receptors results in the phosphorylation of STATs by JAK1 and TYK2. Phosphorylated STATs form protein complexes with each other that migrate into the nucleus, and bind to sites in the promoter regions of ISGs, to initiate transcription of those genes (Platanias, 2005).



Nature Reviews | Immunology

Figure 1. Type I IFN pathway illustration.

The figure summarizes the cascade of molecular events that occur after type I and type II IFN binds to their receptors. The IFN-I receptor is distinguished from the type II receptor by its subunits (IFNAR1/IFNAR2), and the kinases (TYK2/JAK1) associated with the subunits. When the receptors are bound by the appropriate ligands, STAT molecules get phosphorylated, and move into the cell nucleus as dimers where they bind to the genome. ISRE and GAS are sequences that are present in the promoter regions of different interferon stimulated genes (ISGs). (Platanias, 2005).

The differences in the receptors shown in **Figure 1** are what allow for specific targeting of the IFN-I pathway by the compounds we tested. Under normal circumstances, the IFN-I signaling is activated in response to viruses as part of humans' innate immune response. This cascade of events results in the upregulation of immune cell activity to fight off infection (Murira & Lamarre, 2016). However, in patients with neurodegenerative diseases, cdsRNA is constantly present within their neurons, therefore causing chronic neuroinflammation. The inability of immune cells to resolve the inflammatory process may lead to neuronal toxicity and protein aggregation. Immune-related proteins have previously been found in plaques of AD patient brains, serving as evidence that neuroinflammation plays an important role in triggering neurodegeneration (Rahman & Lendel, 2021). This conclusion can also be drawn from a study that found that individuals who take anti-inflammatory drugs had a 50% reduction in the risk of AD development (Zhang et al., 2023). The current understanding is that neuroinflammation is not necessarily a side effect of neurodegeneration, but rather a cause of it.

The mouse line used in this study (Nd1) was genetically engineered to produce cdsRNA in their olfactory neurons. The transgene responsible for the production of cdsRNA selectively in the olfactory neurons of Nd1 mice encodes hAPP gene that has undergone complex rearrangements including an inversion and is under the control of tetracycline response element. Genetic background of

Nd1 is notable for presence of OMP-IRES-TTA transgene, resulting in mature olfactory neuron-selective expression of TTA, a transcription factor that allows for the transcription of the rearranged hAPP transgene by binding to the tetracycline response element. This results in the mature olfactory sensory neuron-selective production of cdsRNA (Rodriguez et al., 2021).

Thus, the cells of interest in this study are mature olfactory sensory neurons (OSNs) because they are the only cells in the Nd1 model that produce cdsRNA. These cells reside in the olfactory epithelium. Every OSN expresses one allele of one odor receptor, making each one responsive to one specific odor. In mice, there are 1000 odorant receptor genes with at least one present on every chromosome (Purves et al., 2001). In OSNs all DNA that codes for any of the odorant receptor genes gets compartmentalized within the nucleus and repressed. Only the odorant receptor gene that is meant to be expressed by a particular OSN then gets unrepressed. Once this is established, the OSN is considered to be mature, and begins to express OMP (**Figure 2**) (McClintock et al., 2020).

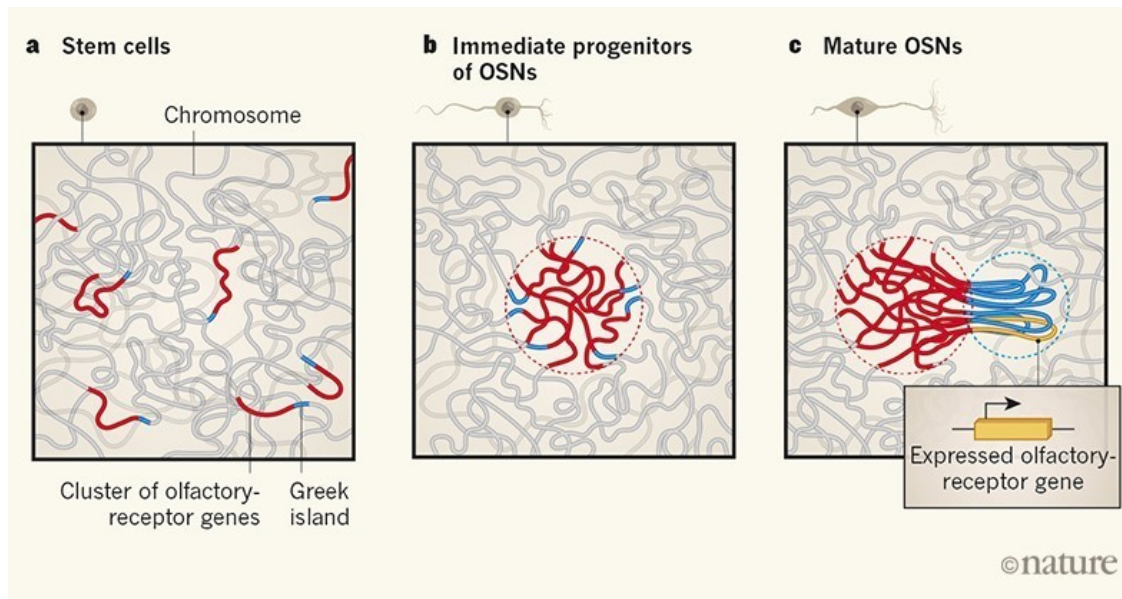


Figure 2. Maturation of olfactory sensory neurons

Repression of all but one odorant receptor gene as an olfactory sensory neuron (OSN) matures. (a) All odorant receptor genes (red) and olfactory-receptor-gene enhancers called Greek islands (blue) are randomly dispersed with all other genetic material within a stem cell. (b) In the immediate progenitors of OSNs all of the odorant receptor genes and Greek islands form an aggregate inside the nucleus that gets repressed. (c) In the mature OSN, only one olfactory receptor gene gets unrepressed (yellow) along with all the Greek islands that enhance its expression. (*Nature News and Views: Chromosomes Come Together to Help Mice Distinguish Odours* | COLUMBIA | Lomvardas Lab, n.d.)

Activation of type I interferon signaling pathway is sometimes strong enough to disrupt the repressed structure inside the OSN nucleus. If this happens, the sense of smell is lost, and can only be regained when the inflammation stops, and the structure can become repressed again. This is why viruses such as SARS-CoV-2, which trigger robust immune responses, can lead to a loss of smell (Rodriguez et al., 2020). This is also why loss of smell is

associated with early onset of neurodegenerative diseases like Alzheimer's (Klein et al., 2021).

TLL041 and TLL082 are TYK2/JAK1 dual kinase inhibitors that may inhibit the inflammatory pathway caused by cdsRNA accumulation (Liang et al., 2023). It is important to note that there may be other neuroinflammatory mechanisms contributing to neurodegeneration. A previous study showed that these drugs have a strong, dose-dependent neuroprotective effect on ReN VM cell-derived human neural cells that have been transfected with double-stranded RNA.

Figure 3 (provided through the courtesy of Laura König from a manuscript that is currently being prepared) shows the cell viability assay and western blot results of this cell study.

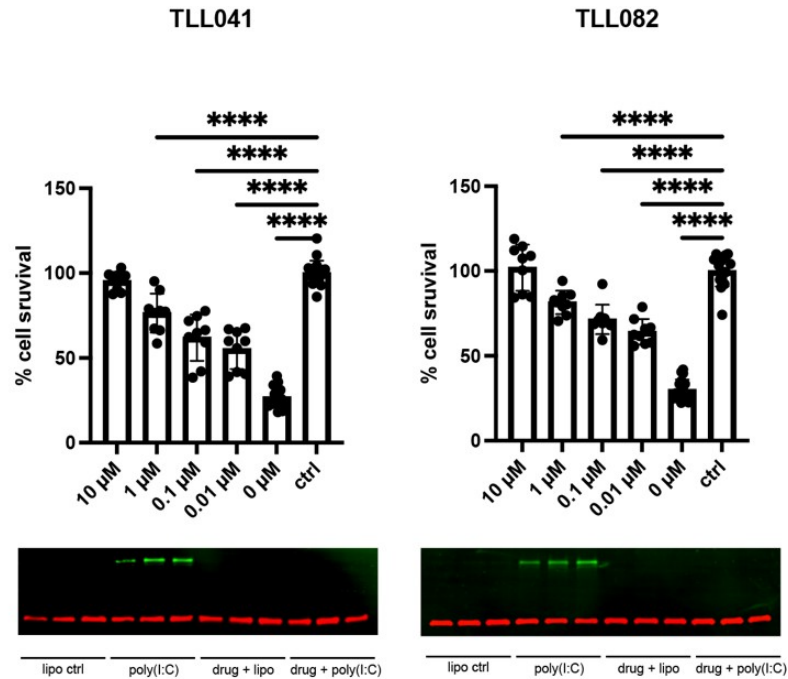


Figure 3. ReN VM cell study results

TLL041 and TLL082 were tested in Ren VM cell-derived human neural cells transfected with dsRNA. For the cell viability assays (bar graphs) the cells were treated at five different concentrations (0, 0.01, 0.1, 1, and 10 μ M) of the compounds. The control bar represents cells that were not transfected with dsRNA (negative control), while the 0 μ M bar represents cells that were transfected with dsRNA, but weren't given any drug (positive control). Cells that were used for western blot analysis (images below bar graphs) were either treated with lipofectamine (vehicle for dsRNA transfection), poly(I:C) (synthetic dsRNA) plus lipofectamine, 10 μ M of drug plus lipofectamine (no dsRNA), or 10 μ M of drug plus lipofectamine and dsRNA. Green and red stains represent p-STAT1 and beta-actin (loading control), respectively.

Based on the cell viability assay results, both compounds seemed to have a dose-dependent effect. At 10 μ M the drugs brought cell viability up to almost 100% like in the negative control cells without dsRNA or drug treatment. As shown by the western blots, the drugs successfully brought down p-STAT1 expression in cells transfected with dsRNA. The assays showed that both

TLL041 and TLL082 were able to rescue cells and diminish type I interferon signaling in vitro.

In this study we tested these compounds on Nd1 mice for their ability to rescue neuronal cell death from the inflammatory effects of cdsRNA accumulation in OSNs and restore the sense of smell.

MATERIALS

MICE

A total of 60 mice were used - 30 females and 30 males (**Table 1**).

Table 1. Disposition of mice across control and experimental groups

30 male (20 Nd1 and 10 BL6) and 30 female (20 Nd1 and 10 BL6) mice received one of five treatments: vehicle, TLL041 at 3.3 mg/kg, TLL041 at 10 mg/kg, TLL082 at 3.3 mg/kg, or TLL082 at 10 mg/kg. Two processing methods were used to analyze mouse tissue after the sacrifice: qPCR or IHC staining. Half of the mice in each group underwent qPCR, and the other half went through immunohistochemistry (IHC) staining.

60 Mice																																			
30 Females										30 Males																									
20 Nd1					10 BL6					20 Nd1					10 BL6																				
4 Vehicle	8 TLL041		8 TLL082		2 Vehicle	4 TLL041		4 TLL082		4 Vehicle	8 TLL041		8 TLL082		2 Vehicle	4 TLL041		4 TLL082																	
	4 3.3 mg/kg	4 10 mg/kg	4 3.3 mg/kg	4 10 mg/kg		2 3.3 mg/kg	2 10 mg/kg	2 3.3 mg/kg	2 10 mg/kg		4 3.3 mg/kg	4 10 mg/kg	4 3.3 mg/kg	4 10 mg/kg		2 3.3 mg/kg	2 10 mg/kg	2 3.3 mg/kg	2 10 mg/kg																
2 qPCR	2 IHC	2 qPCR	2 IHC	2 qPCR	2 IHC	2 qPCR	2 IHC	1 qPCR	1 IHC	1 qPCR	1 IHC	1 qPCR	1 IHC	1 qPCR	1 IHC	1 qPCR	1 IHC	2 qPCR	2 IHC	2 qPCR	2 IHC	2 qPCR	2 IHC	2 qPCR	2 IHC	1 qPCR	1 IHC	1 qPCR	1 IHC	1 qPCR	1 IHC	1 qPCR	1 IHC	1 qPCR	1 IHC

DRUGS

We tested two compounds: TLL041 and TLL082.

METHODS

All mice were at least two months old at the start of the experiment to ensure that their olfactory neurons were mature and producing OMP. Every mouse was put into a separate cage prior to the start of the experiment to keep them from being aggressive towards each other during the dosing.

Both compounds, TLL041 and TLL082, were tested at two different doses in order to test for a dose-dependent effect - 3.3 mg/kg and 10 mg/kg. Each compound was dissolved in 5:95 PEG-300:ddH₂O at a concentration of 0.66 mg/mL for the 3.3 mg/kg dose, or at a concentration of 2 mg/mL for the 10 mg/kg dose. Mice of each sex were divided up into the following groups (Table 1):

- **Positive control group:** 4 Nd1 mice receiving vehicle.
- **Negative control group:** 2 BL6 mice receiving vehicle.
- **Toxicity control groups:** 2 BL6 mice receiving TLL041 at 3.3 mg/kg, 2 BL6 mice receiving TLL041 at 10 mg/kg, 2 BL6 mice receiving TLL082 at 3.3 mg/kg, 2 BL6 mice receiving TLL082 at 10 mg/kg.
- **Experimental groups:** 4 Nd1 mice receiving TLL041 at 3.3 mg/kg, 4 Nd1 mice receiving TLL041 at 10 mg/kg, 4 Nd1 mice receiving TLL082 at 3.3 mg/kg, 4 Nd1 mice receiving TLL082 at 10 mg/kg.

Each mouse was dosed daily for 28 days via oral gavage using a 22 gauge needle and a 1 mL NORM-JECT-F syringe. We used a different needle and syringe for each treatment, one for the vehicle, one for TLL041, and one for TLL082. The mice were weighed once a week to calculate the volume of drug solution to give them, and to track for any weight loss. If any mice dropped to 80% or less of their starting weight, supplements were added to the bottom of their cage. Failure to recover to a healthy weight at the next measurement required the underweight mice to be euthanized.

The volume of treatment given to each mouse via oral gavage was calculated as follows: (weight of the mouse in kg) \times (5 mL/kg). The recommended oral gavage volume for mice ranges from 5-10 mL/kg, so the minimum volume was used.

TLL compounds were dissolved in vehicle (5% PEG-300 in ddH₂O). For complete dissolution of the drugs in the vehicle, every suspension was sonicated for 30 seconds at 4 rms, and then left on a shaker at room temperature overnight at a speed of 1000 rpm. Pure vehicle was kept at 4 °C until dosing. Drug-containing suspensions were made daily because there is no information about how long the TLL compounds stay active in a suspension. To calculate the weight of drug needed for each suspension we did the following:

- **TLL041 3.3 mg/kg:** (sum of all weights of mice receiving this treatment in kg) × (3.3 mg/kg)
- **TLL041 10 mg/kg:** (sum of all weights of mice receiving this treatment in kg) × (10 mg/kg)
- **TLL082 3.3 mg/kg:** (sum of all weights of mice receiving this treatment in kg) × (3.3 mg/kg)
- **TLL082 10 mg/kg:** (sum of all weights of mice receiving this treatment in kg) × (10 mg/kg)

To account for possible oral gavaging error, an extra 0.099 mg of drug was added to the 3.3 mg/kg solutions, and an extra 0.3 mg of drug was added to the 10 mg/kg solutions. The volumes of vehicle added to each treatment were calculated as follows (0.15 mL was added at the end of each formula to account for oral gavaging error):

- **TLL041 3.3 mg/kg:** (sum of all volumes of this treatment given to the mice) + 0.15 mL
- **TLL041 10 mg/kg:** (sum of all volumes of this treatment given to the mice) + 0.15 mL
- **TLL082 3.3 mg/kg:** (sum of all volumes of this treatment given to the mice) + 0.15 mL
- **TLL082 10 mg/kg:** (sum of all volumes of this treatment given to the mice) + 0.15 mL

Perfusion and Dissection:

Mice were sacrificed 2 hours after receiving the last dose of their treatments. To ensure good quality results, all mice were perfused with appropriate buffer to remove blood in the brain tissue. Mice assigned to qPCR analysis were perfused with PBS, and mice assigned to IHC staining analysis were perfused with PBS followed by 4% paraformaldehyde (PFA). Prior to the perfusion, the mice were anesthetized with a ketamine/xylazine cocktail via an IP injection. The cocktail was prepared in 0.9% saline. Drugs were added to the solution so that the ketamine dose was delivered at 100 mg/kg, and the xylazine dose was delivered at 10 mg/kg in each IP injection. The solution was administered at 10 ml/kg of animal. If the animal's pain reflexes did not diminish within 5 minutes, a second dose was administered, and so on until the mouse was fully anesthetized.

All perfusions were completed under a biosafety cabinet. The heart and the liver of the anesthetized mice were exposed by thoracotomy. This was done by making an incision from the lower abdomen of the mouse up to its xiphoid process, making sure to cut through the peritoneum. The diaphragm was cut with scissors, and the ribcage of the mouse was cut laterally so that it could be removed to expose the heart.

A cut was made to their right atria with a small pair of scissors, and a butterfly needle connected to a peristaltic pump with 1 X PBS running through it was stuck into their left ventricles. The peristaltic pump was set to a constant speed of 30 mL/min. Mice in the IHC staining group were also perfused with 4% PFA after PBS using the same method. When the livers of the mice turned pale, and the fluid coming out of the mice was clear the perfusion was considered complete. Mice being perfused with 4% PFA were complete after their legs and tails became stiff from muscle contractions.

After perfusion, we dissected the olfactory epithelia of the mice assigned to qPCR analysis and froze each tissue separately in liquid nitrogen. These samples were placed in the -20 °C fridge for storage before the RNA extraction. Both the olfactory epithelia and olfactory bulbs were dissected out of the mice assigned to IHC staining analysis. Every IHC staining tissue sample was placed into a separate amber vial filled with 4% PFA at 4 °C for an hour. After an hour each tissue sample was put through three 10-minute 1 X PBS washes at 4 °C, and then placed in 0.5 EDTA diluted in 1 X PBS at 4 °C overnight for decalcification.

The day after dissection, IHC samples were placed in 5 mL of 15% sucrose in 1 X PBS for an hour at 4 °C. Each sample was then transferred to 5

mL of 30% sucrose in 1 X PBS overnight at 4 °C. This step was considered complete when the tissue sank in solution. The tissues were allowed to stay in solution for a maximum of 5 days.

Embedding and Sectioning:

After the tissues sank in the 30% sucrose solutions, we embedded the IHC tissue samples in M1 embedding matrix to prepare them for sectioning. First, the samples were placed into embedding molds filled with M1. They were then vacuumed for 30 seconds in a SpeedVac to get out any air bubbles. After the vacuuming step the tissues were frozen in their molds using the following materials:

Dry ice was added to a metal bowl, and isopentane was slowly poured over the dry ice to create a slurry. Inside of the molds with M1, the tissues were positioned to have the rostral side facing down, and the dorsal side facing the notches on the inside of the mold. The molds were then gently lowered into the isopentane, which was filled to a level so that it didn't overflow into the molds. We waited until the M1 turned completely white before taking the molds out of the isopentane, wrapping them with saran wrap, and placing them into the -80 °C fridge.

The samples were kept cold until we sectioned them into 20 μm thick cryosections and placed them onto Super Frost slides for the IHC antibody staining.

RNA Extraction and qPCR:

To complete a qPCR we generated cDNA out of the olfactory epithelia we froze in liquid nitrogen. The first part of generating cDNA required an RNA extraction. All materials for this process came from a QIAGEN RNeasy Mini Kit.

First, we manually homogenized each tissue sample in 600 μL of Buffer RLT. We then centrifuged the lysate for 3 minutes at 15000 rpm (maximum speed) and removed the supernatant by pipetting to be used in the next step. We added 600 μL of 70% ethanol to the supernatant from each sample and mixed everything together by pipetting. Seven hundred μL of each sample (including precipitate) was transferred to RNeasy Mini spin columns placed in 2 mL collection tubes. We centrifuged all tubes for 15 seconds at 15000 rpm and discarded the flow-through.

The next steps were taken for DNase digestion to remove possible DNA contamination in our RNA samples. We added 350 μL of Buffer RW1 to each RNeasy column and centrifuged for 15 seconds at 15000 rpm. The flow-through

was discarded. The next step required the preparation of a DNase I stock solution. This was made by adding 550 μL RNase-free water into the DNase I vial provided by the kit. Next, we prepared a 1:7 DNase I incubation mix using the DNase I stock solution and Buffer RDD, respectively. We briefly centrifuged this mixture before moving on to the next step. 80 μL of the centrifuged incubation mix was added to each RNeasy column membrane, and left at room temperature for 15 min. Finally, 350 μL of Buffer RW1 was added to each RNeasy column and centrifuged once again at 15000 rpm for 15 seconds. We resumed the RNA purification process after discarding the flow-through produced by the spin-down.

The last few steps were a series of spin-downs. We added 500 μL of Buffer RPE to each RNeasy spin column and centrifuged for 15 seconds at 15000 rpm, getting rid of any flow-through at the end. We repeated the addition of 500 μL of Buffer RPE to each spin column, but this time we centrifuged for 2 minutes at 15000 rpm. In the last step the Rneasy spin columns were placed in new 1.5 mL collection tubes, and 40 μL pf RNase-free water was added directly to the spin column membrane. This was centrifuged for 1 min at 15000 rpm to elute the final RNA product.

Before generating cDNA from the RNA, we measured the RNA content from each tissue sample using a spectrophotometer. Ideally, RNA concentrations

should have been 100 ng/uL or more, but many were under 100 ng/uL, so we attempted to do an RNA cleanup on two samples to see if we could get a higher RNA yield.

For the RNA cleanup we first adjusted our sample volumes to 100 uL by adding more nuclease-free water. We diluted the RNA further by adding 250 uL of 96-100% ethanol and mixed well. Then, we transferred 700 uL of each of the samples into two RNeasy mini spin columns placed in 2 mL collection tubes. We centrifuged the spin columns for 15 seconds at 15000 rpm, and then discarded the flow-through. Next, we added 500 uL of Buffer RPE to each spin column, and centrifuged again for 15 seconds at 15000 rpm, discarding the flow-through once again. We repeated this step again but centrifuged for 2 minutes instead of 15 seconds. After the second spin-down, we placed the mini spin columns into new 1.5 mL collection tubes and added 30 uL of RNase-free water directly to the spin column membranes. Once again, we centrifuged the samples for 1 minute at 15000 rpm. We kept the flow-through and measured the RNA concentrations again using a spectrophotometer. All samples were placed into the -20 °C fridge for storage.

We proceeded to generate the cDNA from the extracted RNA. First, we prepared a genomic DNA digestion reaction mix for each sample to get rid of any DNA that could have been contaminating our extracted RNA. We used the RNA

concentration values from the spectrophotometer to calculate how much RNA was to be added to each mix to get 1 ug of RNA per 10 uL of reaction. 1 uL of 10 X ezDNase Buffer and 1 uL of ezDNase enzyme was added to every sample, and then nuclease-free water was added as needed to bring the total reaction mix volume up to 10 uL. For RNA concentrations under 100 ng/uL we ended up adding 8 uL of extracted RNA to the reaction mixture, and no nuclease-free water. These reaction mixtures were then mixed and incubated at 37 °C for 2 minutes. After the 2-minute incubation step, the samples were cooled down to room temperature on ice, and briefly centrifuged before being placed back on the ice.

Next, we annealed the primers to our template RNA. 9 uL of template RNA was used for each mixture, and 1 uL of 50 ng/uL random hexamers, 1 uL of 10 mM dNTP mix, and 2 uL of DEPC-treated water were added. All components were mixed, and briefly centrifuged. Then we heated the RNA-primer mixes at 65 °C for 5 minutes, and afterwards put them back on ice for at least 1 minute.

We prepared a reverse transcriptase reaction mix to be added in 7 uL volumes to every sample. 4 uL of 5 X SSIV buffer, 1 uL of 100 mM DTT, 1 uL of ribonuclease inhibitor, and 1 uL of SSIV reverse transcriptase made up each 7 uL volume.

We added the reverse transcriptase reaction mix to every sample, and then proceeded to do a series of incubations. First, we held the sample at 23 °C for 10 minutes, then at 53 °C for another 10 minutes, and lastly at 80 °C for a final 10 minutes. We used a spectrophotometer to record the cDNA concentrations and kept the samples at -20 °C until the qPCR.

The goal of the qPCR was to test for inflammatory marker levels including IFN- γ , IL-6, IL-17A, TNF- α , CXCL10, CCL2, MDA5, STAT1, OASL2, and neuronal death markers like NFL and tau. The control marker was the glycolytic enzyme, GAPDH, present in all cells.

The first step of the qPCR was making a 1:10 dilution with each cDNA sample using nuclease-free water. These dilutions were kept on ice with all the primers and SYBR green. All the next steps were completed under a hood to avoid contamination, since this assay is extremely sensitive. For each primer, a master mix was made to contain 5 μ L of SYBR green, 0.3 μ L of primer (forward and reverse), and 3.7 μ L of nuclease-free water per 10 μ L of reaction. To figure out how much of each master mix component was needed for each master mix, all numbers were multiplied by the number of samples (+3) to account for pipetting error.

The 96-well plate was set up in such a way so that each primer had two replicates. The outermost wells around the border of the plate were not used to test the samples in order to avoid contamination.

Table 2. qPCR 96-well Plate Setup

Each cell in this table represents a well on the 96-well plate (in the top row some of the cells were merged, but there technically are 12 wells). The outermost borders (except the last row) were wells left empty on the plate, and they were either labeled to indicate what went into each of the other wells (top row and left column), or just left blank (right column). For each primer and cDNA sample combination there were two replicates as indicated by wells labeled “R.1” and “R.2”. The bottom row of the plate was used as a control for the primers, so no cDNA was added to the wells, only the master mix. Cells labeled “Blank” had no master mix added to them because there was no need for replicates in the control row. Cells labeled “Master” had master mix added to them.

	Primer 1		Primer 2		Primer 3		Primer 4		Primer 5		
DNA Template 1	R.1	R.2	R.1	R.2	R.1	R.2	R.1	R.2	R.1	R.2	
DNA Template 2	R.1	R.2	R.1	R.2	R.1	R.2	R.1	R.2	R.1	R.2	
DNA Template 3	R.1	R.2	R.1	R.2	R.1	R.2	R.1	R.2	R.1	R.2	
DNA Template 4	R.1	R.2	R.1	R.2	R.1	R.2	R.1	R.2	R.1	R.2	
DNA Template 5	R.1	R.2	R.1	R.2	R.1	R.2	R.1	R.2	R.1	R.2	
DNA Template 6	R.1	R.2	R.1	R.2	R.1	R.2	R.1	R.2	R.1	R.2	
No cDNA Controls	Blank	Master	Blank	Master	Blank	Master	Blank	Master	Blank	Master	

9 μ L of master mix and 1 μ L of cDNA sample was added into their corresponding wells. Afterwards, a microseal was gently placed over the plate.

The qPCR plate was then centrifuged at 500 rpm for a minute before being placed into a thermal cycler to generate results. The thermal cycler has an initial 3-minute heating period up to 95 °C, and then 40 rounds of a 10 second denaturation step at 95 °C followed by a 30 second reannealing step at 55 °C. After the 40 cycles of denaturation and reannealing, the plate is kept at 55 °C for another 30 minutes before completion.

qPCR Statistical Analysis:

Cq values obtained from qPCR were converted to raw gene expression numbers by the following formula: $1/2^{Cq}$. We omitted all Cq values under 20 to exclude any possible outliers in our dataset. This value was chosen because all GAPDH Cq values in our control groups were higher than 20, and all other markers were expressed at lower levels (higher Cq numbers) than GAPDH. GAPDH raw gene expression thus obtained was used to normalize the raw gene expression of STAT1, MDA5, IFI44, and OASL2. Mean of normalized gene expression of each of the above genes per mouse was calculated (number of measurements per mouse ranged from 1 to 6). Subsequently, mean expression numbers of Nd1 experimental groups were compared to Nd1 vehicle group using Welch t-test. Same was done for BL6. Boxplots were constructed using normalized raw gene expression values described above.

Antibody Retrieval and IHC Antibody Staining:

Since our IHC tissue samples were preserved using 4% PFA, we performed antigen retrieval before moving on to the staining to ensure that the antibodies are able to detect our proteins of interest.

We made 10 mM sodium citrate by dissolving 2.94 g of tri-sodium citrate in 1 L of distilled water, and then adjusting the pH to 6 with 1M HCl. To finish making the sodium citrate buffer we added 0.05 mL of tween 20 and mixed well.

We placed the SuperFrost slides into slide holders filled with water for 3 minutes, and microwaved other slide holders filled with our sodium citrate buffer for 45 seconds, or until it began to bubble. After 3 minutes of being submerged in water, we moved the slides to the slide holders with the heated buffer and placed them in a steamer for 30 minutes. After that, we allowed the slides to cool for 20 minutes. At this point, the antigen retrieval was complete.

The staining was a two-day process. On the first day we started by fixing all of the sections in 4% PFA for 15 minutes. We then washed off the 4% PFA by putting all slides through three 3-minute 1X PBS washes. After every wash, the slides were dabbed on a kim wipe to remove excess liquid. Next, we put the slides inside incubation chambers covered with tinfoil and used about 200 μ L of

blocking buffer per slide, making sure to distribute the volume evenly between all sections on the slides. The blocking buffer was made using 5% normal serum, and 0.1% Triton X in PBS. This step was done for an hour. We then distributed 200 uL of primary antibody dissolved in blocking buffer over each slide. The antibodies we used were for CCasp3 (marker of cell death), OMP, γ H2AX, STAT1, and MDA5. Hybri slips were added to the slides and kept overnight inside incubation chambers placed in the 4 °C fridge.

On day two of the staining process, we first removed the hybri slips from the slides by immersing them in PBS. Then, we proceeded to wash the slides 3 times in PBS for 3 minutes. After each wash, the excess liquid on the slides was dried with a kim wipe. Secondary antibody dissolved in blocking buffer was then added in a volume of 150-200 uL to each slide. The slides were kept at room temperature for 1-2 hours inside their incubation chambers. The slides were washed again 3 times in PBS to remove the secondary antibody, keeping them isolated from light during the washes. Finally, 200 uL of DAPI glycerol solution was added to each slide. Glass coverslips were placed over the slides, ensuring that no bubbles formed underneath. The slides were then imaged using a microscope.

RESULTS

The experiments were carried out using 55 of the 60 planned mice. The five mice that weren't used were either too young at the start of the experiment or were in a mating. These mice will be treated separately from the rest of the mice once they are old enough or have given birth to their pups. Four of the five missing mice were females in the "Nd1 mice receiving 10 mg/kg TLL082" group, and the other mouse was a female in the "Nd1 mice receiving 3.3 mg/kg TLL082" group.

Mouse weights were recorded weekly to check if the drug had any toxic side effects. **Figure 4** shows the weight fluctuations in the mice over the 4 weeks of treatment.

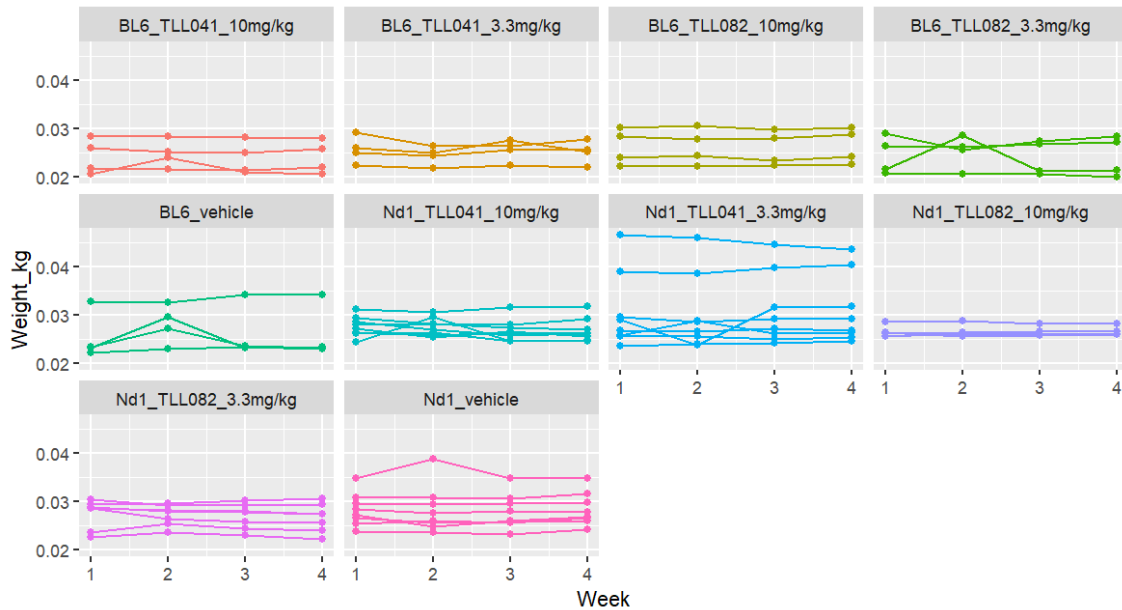


Figure 4. Mouse weights over treatment period

Graph represents the weights of mice in 10 different treatment groups (one group per panel) over the four-week (28 days) course of treatment. Every line tracks the weight of an individual mouse. Weights were recorded on day 1 of weeks 1, 2, 3, and 4.

The treatment course lasted four weeks. Upon completion of the treatment all mice were sacrificed. An RNA extraction was performed on olfactory epithelia of mice that were perfused with 1 X PBS. cDNA was generated from the extracted RNA.

Table 3 shows the results of both the RNA extraction, and cDNA generation.

Table 3. RNA/cDNA Counts and Ratios

Column 1 of this table shows the mouse IDs. Columns 2-4 show the concentration of RNA in each sample, the optical density 260 nm/230 nm and the 260 nm/280 nm nucleic acid purity ratio for the RNA. Columns 5-7 show the concentration of cDNA in each sample, the optical density 260 nm/230 nm nucleic acid purity ratio for the cDNA, and the 260 nm/280 nm nucleic acid purity ratio for the cDNA. The rightmost column shows the ratio of RNA:cDNA for each sample.

Mouse ID	RNA (ng/uL)	OD 260/230	OD 260/280	cDNA (ng/uL)	OD 260/230	OD 260/280	RNA:cDNA Ratio
1754.6-0	20.946	0.147	1.660	762.209	1.39	1.72	See table 4
1754.6-2	52.487	1.216	1.976	1110.209	1.38	1.79	0.047
1751.2-0	27.507	0.361	2.001	1267.644	1.23	1.65	0.022
1690.2-2	19.039	0.122	1.902	1288.404	1.42	1.78	See table 4
1678.1-0	63.895	1.021	2.031	1334.708	1.17	1.67	0.048
1690.5-1	33.004	0.304	1.938	1040.297	1.40	1.80	0.032
1754.6-4	34.985	0.611	1.882	1173.182	1.34	1.77	0.030
1761.2-1	70.040	0.940	1.953	1070.456	1.45	1.77	0.065
1736.2-5	61.118	0.883	1.993	1225.480	1.51	1.80	0.050
1730.4-1	51.548	0.718	1.962	1062.161	1.41	1.77	0.050
1758.2-5	52.752	0.499	2.059	1111.472	1.37	1.76	0.047
1751.3-0	44.883	0.362	1.896	1218.719	1.44	1.79	0.037
1761.2-3	180.810	2.006	2.081	1001.617	1.53	1.78	0.181
1761.2-5	174.364	1.231	2.100	1254.693	1.47	1.80	0.139
1750.3-5	49.788	1.251	1.978	1278.926	1.46	1.79	0.039
1719.5-4	72.881	0.954	2.081	715.621	1.51	1.80	0.102
1751.3-2	57.450	0.368	1.864	1086.585	1.38	1.76	0.053
1751.1-1	63.694	0.555	1.952	884.951	1.43	1.77	0.072
1761.2-7	40.120	0.401	2.024	1122.700	1.42	1.77	0.036
1761.3-0	60.232	0.641	1.922	1064.964	1.42	1.77	0.057
1750.5-0	145.263	1.036	1.973	1231.551	1.47	1.79	0.118

1750.4-5	38.180	0.364	1.888	1096.051	1.43	1.78	0.035
1751.3-1	71.377	0.507	1.977	1076.148	1.38	1.77	0.066
1758.3-4	84.326	1.238	1.950	1236.975	1.51	1.80	0.068
1761.3-2	50.992	0.497	1.859	886.403	1.41	1.80	0.058
1761.3-4	44.854	1.109	1.868	1171.034	1.55	1.78	0.038
1750.5-3	151.471	1.228	2.087	1269.952	1.54	1.80	0.119
1750.4-0	146.636	1.416	2.058	1131.715	1.57	1.79	0.130

The ideal RNA concentration value after an RNA extraction should be >100 ng/uL. Many of the samples ended up with values < 100 ng/uL, so the RNA had to be repurified. Two samples were tested to see if RNA concentrations improved. The results are shown in Table 4.

Table 4. RNA/cDNA Counts and Ratios after RNA repurification

Two samples were selected for the RNA cleanup to check if the RNA yield improved. The leftmost column of this table shows the mouse IDs that were selected for this process. Columns 2-4 show the concentration of RNA in each sample, the 260/230 nucleic acid purity ratio for the RNA, and the 260/280 nucleic acid purity ratio for the RNA after cleanup. cDNA was obtained from these samples after the cleanup. Columns 5-7 show the concentration of cDNA in each sample, the 260/230 nucleic acid purity ratio for the cDNA, and the 260/280 nucleic acid purity ratio for the cDNA. The rightmost column shows the ratio of RNA:cDNA for each sample.

Mouse ID	RNA (ng/uL)	OD 260/230	OD 260/280	cDNA	OD 260/230	OD 260/280	RNA:cDNA Ratio
1754.6-0	16.955	0.365	2.364	762.209	1.39	1.72	0.022
1690.2-2	20.844	0.295	1.943	1288.404	1.42	1.78	0.016

RNA concentrations of the two samples in **Table 4** did not improve from the RNA repurification so the rest of the samples were made into cDNA after the first RNA extraction.

After generating cDNA from every olfactory epithelium sample, we ran a qPCR analysis on half of the mice from every treatment group. **Table 5** shows the mean inflammatory marker expression in each group, and the statistical significance of the results.

Table 5. Treatment group inflammatory marker expression and p-values

Values for inflammatory markers STAT1, MDA5, IFI44, and OASL2 are shown in the third column for each treatment group. The p-values and 95% confidence intervals are from Welch Two Sample t-test comparing vehicle to respective treatment groups per mouse model (BL6 or Nd1). All p-values < 0.05 shown in red are considered to be significant. Fold change of expression from baseline is shown in the fifth column. T-test results for IFI44 are pending for all BL6 groups.

Treatment Group	Inflammatory Marker	Mean Expression	Confidence Interval (95%)	Fold Change of Expression from Baseline	p-value
BL6 + Vehicle	STAT1	5.64E-03	N/A	N/A	N/A
	MDA5	6.26E-03	N/A	N/A	N/A
	IFI44	N/A	N/A	N/A	N/A
	OASL2	1.57E-02	N/A	N/A	N/A
BL6 + TLL041 3.3 mg/kg	STAT1	7.03E-03	-0.01025264 ; 0.00747893	1.25E+00	4.72E-01
	MDA5	5.79E-03	-0.02354465 ; 0.02448427	9.25E-01	8.87E-01
	IFI44	N/A	N/A	N/A	N/A
	OASL2	1.04E-02	-0.03084976 ; 0.04136674	6.65E-01	4.06E-01
BL6 + TLL041 10 mg/kg	STAT1	1.05E-02	-0.03471242 ; 0.02495706	1.86E+00	3.85E-01
	MDA5	1.01E-02	-0.01835608 ; 0.01064904	1.62E+00	2.57E-01
	IFI44	N/A	N/A	N/A	N/A
	OASL2	1.34E-02	-0.02390857 ; 0.02848385	8.54E-01	6.84E-01
BL6 + TLL082 3.3 mg/kg	STAT1	1.70E-02	-0.1622902 ; 0.1395689	3.01E+00	5.28E-01
	MDA5	6.63E-03	-0.009699407 ; 0.008966987	1.06E+00	7.21E-01
	IFI44	N/A	N/A	N/A	N/A
	OASL2	1.61E-02	-0.08133031 ; 0.08042924	1.03E+00	9.73E-01
BL6 + TLL082 10 mg/kg	STAT1	9.21E-03	-0.02009081 ; 0.01294666	1.63E+00	2.23E-01
	MDA5	1.11E-02	-0.011295046 ; 0.001681203	1.77E+00	7.27E-02
	IFI44	N/A	N/A	N/A	N/A
	OASL2	5.38E-03	-0.01342849 ; 0.03405004	3.43E-01	1.89E-01
Nd1 + Vehicle	STAT1	6.08E-02	N/A	N/A	N/A
	MDA5	3.81E-02	N/A	N/A	N/A
	IFI44	2.18E-03	N/A	N/A	N/A
	OASL2	5.50E-01	N/A	N/A	N/A
Nd1 + TLL041 3.3 mg/kg	STAT1	1.37E-02	0.02388016 ; 0.07038302	2.25E-01	5.87E-03
	MDA5	8.86E-03	0.01638626 ; 0.04202201	2.33E-01	3.00E-03
	IFI44	1.48E-05	0.0021808190 ; 0.0000147703	6.77E-03	4.38E-03

	OASL2	2.48E-02	0.2956094 ; 0.7555598	4.51E-02	5.26E-03
Nd1 + TLL041 10 mg/kg	STAT1	4.91E-02	-0.04837319 ; 0.07188378	8.07E-01	6.12E-01
	MDA5	2.81E-02	-0.01854552 ; 0.03844778	7.39E-01	3.92E-01
	IFI44	1.17E-03	-0.0007017975 ; 0.0027245420	5.36E-01	1.82E-01
	OASL2	2.04E-01	0.01225782 ; 0.68108100	3.70E-01	4.46E-02
Nd1 + TLL082 3.3 mg/kg	STAT1	6.55E-02	-0.1459646 ; 0.1365667	1.08E+00	9.24E-01
	MDA5	6.79E-02	-0.1870003 ; 0.1274050	1.78E+00	5.91E-01
	IFI44	1.91E-03	-0.003282262 ; 0.003815942	8.78E-01	8.35E-01
	OASL2	3.63E-01	-0.7982831 ; 1.1723639	6.82E-01	6.03E-01
Nd1 + TLL082 10 mg/kg	STAT1	5.33E-02	-0.4185092 ; 0.4335212	8.77E-01	8.79E-01
	MDA5	3.22E-02	-0.1210489 ; 0.1328417	8.45E-01	7.46E-01
	IFI44	1.41E-03	-0.01229519 ; 0.01383194	6.48E-01	6.47E-01
	OASL2	8.95E-02	0.08676668 ; 0.83499243	1.63E-01	3.08E-02

The results shown in **Table 5** are visualized using box plots.

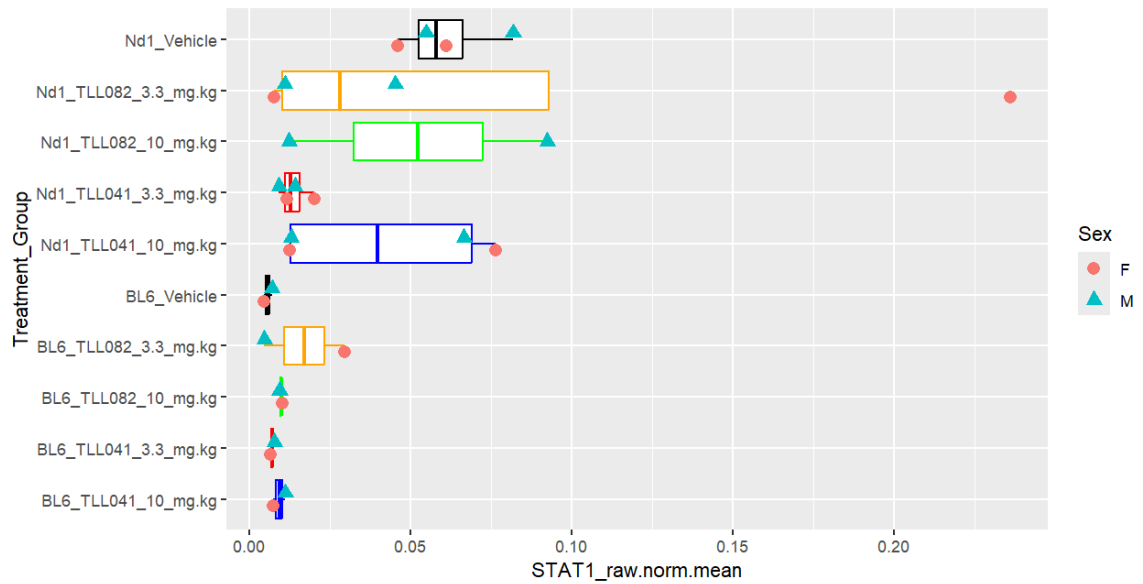


Figure 5. STAT1 gene expression

Gene expression levels for STAT1 for every mouse in each treatment group were plotted. Treatment groups are indicated on the vertical axis of the plot. Males and females are shown as green triangles and red circles, respectively. X axis values are normalized gene expression to that of GAPDH.

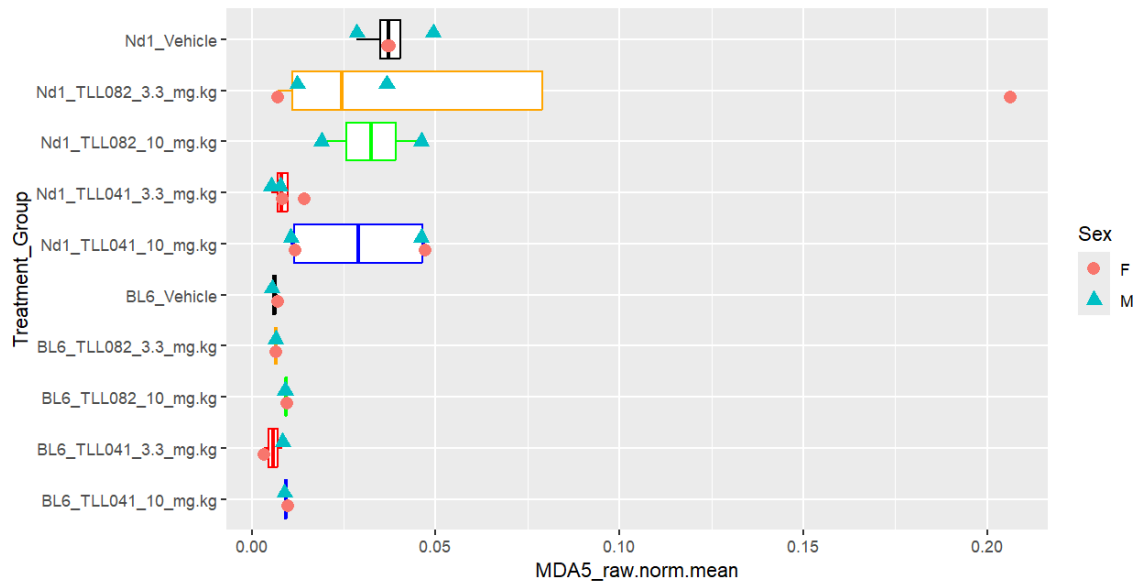


Figure 6. MDA5 gene expression

MDA5 gene expression levels for every mouse in each treatment group were plotted. Treatment groups are indicated on the vertical axis of the plot. Males and females are shown as green triangles and red circles, respectively. X axis values are normalized gene expression to that of GAPDH.

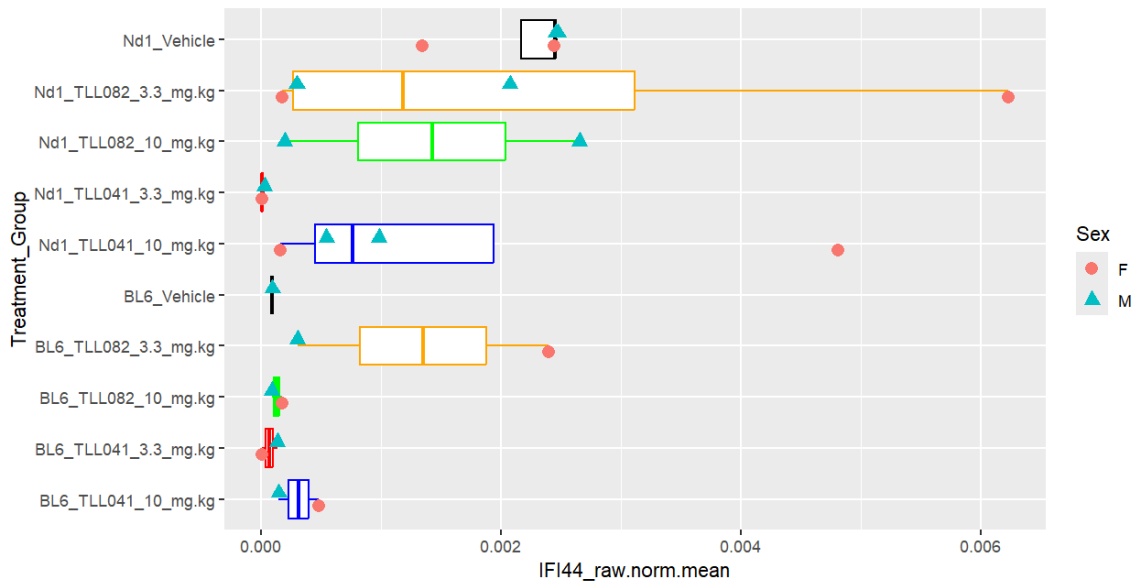


Figure 7. IFI44 gene expression

IFI44 gene expression levels for every mouse in each treatment group were plotted. Treatment groups are indicated on the vertical axis of the plot. Males and females are shown as green triangles and red circles, respectively. X axis values are normalized gene expression to that of GAPDH.

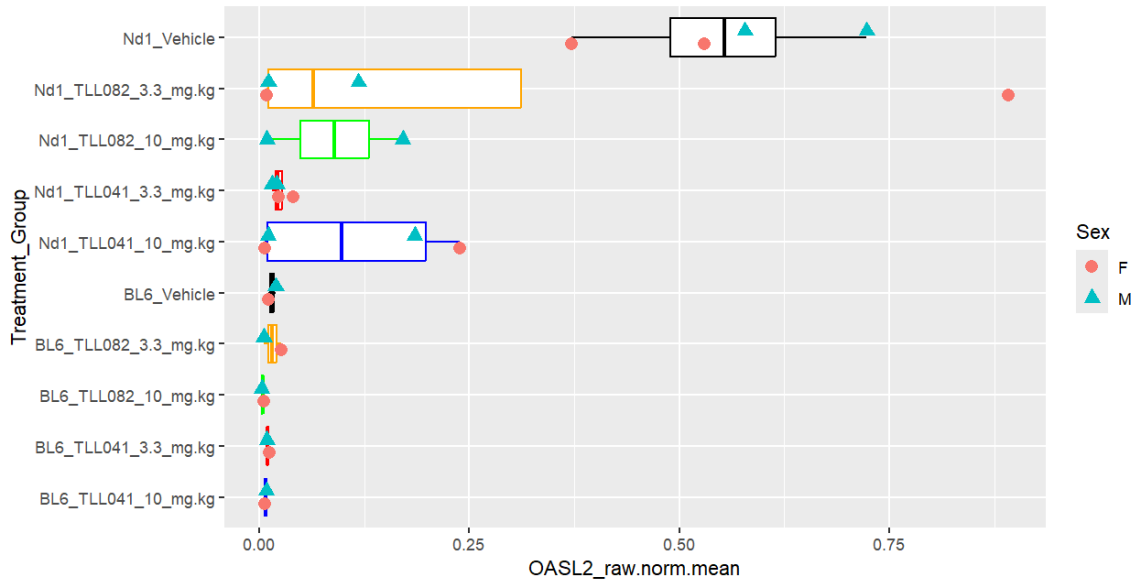


Figure 8. OASL2 gene expression

OASL2 gene expression levels for every mouse in each treatment group were plotted. Treatment groups are indicated on the vertical axis of the plot. Males and females are shown as green triangles and red circles, respectively. X axis values are normalized gene expression to that of GAPDH.

qPCR results for the remaining inflammatory markers, and IHC antibody staining results are pending.

DISCUSSION

Two compounds, TLL041 and TLL082, were tested on neurodegenerative mouse models to see if inhibiting the TYK2/JAK1 kinases in the type I interferon pathway is an effective method at diminishing neuroinflammation leading to neuronal rescue. cdsRNA is thought to be the cause of the IFN-I pathway activation in the neurons of patients with diseases such as Alzheimer's disease, frontotemporal dementia, and ALS. The Nd1 mice used in our study produce cdsRNA in their olfactory neurons to mimic the effects of neurodegeneration. We dosed the mice daily for 28 days with the Biohaven compounds, and then analyzed their olfactory epithelia and olfactory bulbs with qPCRs and IHC antibody stainings to assess the efficacy of these drugs. We hypothesized that both compounds would inhibit the IFN-I signaling pathway and show a dose-dependent effect.

During the treatment period, we recorded the weights of our mice weekly in order to see if the compounds had any toxic effects. As depicted in **Figure 4**, neither TLL041 nor TLL082 had any effect on the mice's weight suggesting that the drugs did not exert toxic side effects. The weights of all mice stayed constant over the treatment course. Every new weight that was recorded was compared to the weights obtained in week 1 to make sure that mouse weight didn't drop below 85% of the starting weight. However, the week 2 weight obtained for mouse

1736.2-5 was found to be 81% of its original weight. Nutritional supplements were added into the mouse's cage, and the mouse's weight went back to normal by the week 3 weigh-in. Since none of the other mice experienced a >15% weight drop at any point during the treatment course, we assumed that the weight loss was not significant to be indicative of toxic drug effect.

After sacrificing all mice, half of the olfactory epithelium samples were used for an RNA extraction so that we could make cDNA to run qPCRs. **Table 3** shows the final RNA concentrations based on optical density. Ideally, we wanted to obtain RNA concentrations of at least 100 ng/uL. However, as shown in **Table 3**, only five of the 28 samples ended up with ideal RNA concentrations. We suspect that the rest of the samples had lower concentration values because of poor homogenization in the first step of the RNA extraction. Incomplete disruption of tissue results in inefficient release of RNA into the lysate, resulting in yields that were lower than expected. We homogenized our tissues manually using a pestle, and then briefly vortexing the tissue bits. In the future we will attach the pestle to a motor adaptor for better homogenization and higher RNA yield.

The 260 nm/280 nm ratios for RNA shown in **Table 3** indicated the purity of the extraction. By itself, RNA has an absorbance of 260 nm. RNA is considered pure when the 260 nm/280 nm ratio is ~2. The majority of our values ranged from 1.8-2.1, with the exception of sample 1754.6-0, which had a ratio of

1.660. Lower 260 nm/280 nm ratios are typically a result of contaminants with a 280 nm absorbance in the RNA extraction sample. Examples of such contaminants are proteins and phenols. In the future, an additional chloroform wash could be included to attempt to remove such contaminants.

A secondary measure of RNA purity is the 260 nm/230 nm ratio. These values were also included in **Table 3**. Pure RNA is considered to have a 260 nm/230 nm ratio of ~2. Lower values indicate contamination with salts, carbohydrates, peptides, or phenols. Only sample 1761.2-3 had a ratio of ~2 indicating RNA purity. All other values were indicative of contamination, most likely with guanidine thiocyanate, a compound present in lysis buffers in commercial RNA extraction kits such as the one we used.

Due to low RNA concentration yields in the majority of our samples, we picked two samples for RNA cleanup process to check if RNA yield improved. Based on the spectrophotometer results shown in **Table 4**, there wasn't a significant change in RNA concentration, although the 260 nm/280 nm ratio of sample 1754.6-0 went up from 1.660 to 2.364, meaning the purity of RNA improved. We decided against doing the RNA cleanup on the rest of our samples because their 260 nm/280 nm ratios were already ~2, and we didn't want to risk losing RNA following further purification steps.

After generating cDNA from our extracted RNA, we determined the level of cDNA by optical density as shown in tables 3 and 4. All of our RNA:cDNA ratios were lower than 1 due to the fact that random hexamer primers were used to produce cDNA from our extracted RNA, producing multiple varying length fragments of cDNA from each RNA. Because our starting RNA concentrations were lower than expected, using random hexamers was actually beneficial because we were able to achieve high cDNA yields.

The normal 260 nm/280 nm ratio value for dsDNA ranges from 1.7-2. Based on the cDNA 260 nm/280 nm ratios, the samples were all pure with the exception of sample 1751.2-0. This was likely due to the presence of contaminants listed previously in the discussion of RNA purity. All 260 nm/230 nm ratios for cDNA were below the normal range of 2-2.2. As mentioned previously, guanidine thiocyanate was the likely cause of the lower than normal ratios because its absorbance is 230 nm, and it is commonly used in column based kits.

Using the cDNA that we generated we were able to run qPCRs to determine the gene expression levels of GAPDH, STAT1, MDA5, IFI44, and OASL2. GAPDH is a metabolic enzyme present in all cells, and we used its expression levels to normalize the rest of our results. In the last row of our qPCR plates we only put the primers into the wells without any cDNA. This was to test

for any potential DNA contamination in our primers that might skew our results. Some bottom row wells did end up having Cq values, but the replicates were drastically different so we assume that the contamination was on the plate rather than the actual primers. Also, the same primer stock was used daily to prepare the master mixes, and on some of the days the wells did not generate Cq values. Contamination is very common in qPCRs when the edges of the plate are used, so to avoid generating Cq values for our control wells in the future we will use the second to last row of the plate instead of the last row.

We expected that the BL6 mice receiving drug would have p-values >0.05 for all inflammatory markers, assuming that both drugs are non-toxic. As shown in **Table 5**, the results matched our expectations for STAT1, MDA5, and OASL2. We were unable to run a t-test on IFI44 for the BL6 groups because our “BL6 + vehicle” group had qPCR results for only one of the two mice. We will need to run another qPCR for the missing sample before we are able to check for a significant difference in IFI44. Raw Cq value results for IFI44 in all BL6 mice look very similar so we are expecting the p-value for this inflammatory marker to also be >0.05 once we run a t-test. STAT1, MDA5, and OASL2 expression level data serves as further evidence in addition to mouse weight data that the drugs do not have any toxic side effects that might elevate inflammatory marker levels in our other experimental groups.

The Nd1 mice receiving vehicle served as our positive control group, and we expected to see comparatively higher levels of inflammation in this group than in the BL6 mice receiving vehicle (our negative control). In **Figures 5-8** there is a clear depiction of all inflammatory marker levels being higher in Nd1 mice receiving vehicle than in BL6 mice receiving vehicle, serving as evidence that our mouse model produces a neuroinflammatory response.

For the Nd1 mice receiving drug, we expected to see a drop in inflammatory marker expression compared to the positive control if TYK2/JAK1 were in fact inhibited. In the “Nd1 + TLL041 3.3 mg/kg” treatment group all inflammatory marker expression levels dropped significantly as shown by the p-values in **Table 5** (STAT1:5.87E-03, MDA5:3.00E-03, IFI44:4.38E-03, OASL2: 5.26E-03), indicating that TLL041 was effective at inhibiting neuroinflammation when administered at 3.3 mg/kg. The boxplots for the “Nd1 + TLL041 3.3 mg/kg” treatment group in **Figures 5-8** are also visibly more similar to the boxplots for BL6 mice receiving vehicle than to the boxplots for Nd1 mice receiving vehicle. This means that TLL041 was able to significantly reduce inflammation levels in Nd1 mice almost to the baseline levels seen in our negative control BL6 mice.

We expected to see a similar, or even greater decrease in inflammatory marker expression levels for TLL041 at a dose of 10 mg/kg. This would align with the results of the cell study shown in **Figure 3**. However, as shown in **Table 5**,

the only inflammatory marker that decreased significantly was OASL2. Interestingly, the mean expression of OASL2 in the group receiving 10 mg/kg of TLL041 was greater than the mean expression of the same marker in the group receiving 3.3 mg/kg of TLL041. Also, although the change in expression levels for the markers STAT1, MDA5, and IFI44 were not significant in the “Nd1 + TLL041 10 mg/kg” group, there was still a decrease in expression for all markers based on the “fold change in expression from baseline” values in **Table 5** (STAT1:8.07E-01, MDA5:7.39E-01, IFI44:5.36E-01). In **Figures 5-8** the boxplots for the “Nd1 + TLL041 10 mg/kg” group show an interesting distribution with two of the mice always having expression values closer to the “Bl6 + vehicle” group, and two of the mice always having expression values closer to the “Nd1 + vehicle” group. This likely means that the drug was effective in only two of the four mice in this group. A possible explanation for these results is that the drug did not get fully dissolved in the vehicle at this dose, and some of the mice were therefore unable to properly digest the compound so that it got to the brain. To avoid this issue in the future we can either try to dissolve the drug in a larger volume of the vehicle we used in this study, or we can try to find a different vehicle so that we don't have to risk giving the mice a larger volume than their stomachs can hold.

The “Nd1 + TLL082 3.3 mg/kg” qPCR results were expected to be similar to the results we obtained for TLL041 at the 3.3 mg/kg dosage. Surprisingly, we

found that there were no statistically significant differences for any of the inflammatory markers. According to **Table 5** STAT1 and MDA5 had a fold increase (STAT1:1.08E+00, MDA5:1.78E+00) compared to controls, and IFI44 and OASL2 had a fold decrease (IFI44:8.78E-01, OASL2:6.82E-01), although all of these changes were not statistically significant. In the boxplots for this group shown in **Figures 5-8** a similar distribution to the “Nd1 + TLL041 10 mg/kg” is seen. Two of the mice consistently expressed all inflammatory markers at similar levels to the “BL6 + vehicle” group indicating that TLL082 might have worked in them at a dose of 3.3 mg/kg. The other two mice in this group showed values closer to “Nd1 + vehicle” expression levels for all inflammatory markers suggesting that the drug did not work.

In the “Nd1 + TLL082 10 mg/kg” group only OASL2 expression levels were significantly decreased compared to the “Nd1 + vehicle” group. These results are similar to the “Nd1 + TLL041 10 mg/kg” group. The rest of the inflammatory markers all showed a fold decrease, but these results were not significant. The “Nd1 + TLL082 10 mg/kg” group only had two mice because we didn't have enough mice that were old enough to treat. In the boxplots for inflammatory markers STAT1, MDA5, and IFI44 (**Figures 5-7**), one of the mice in this group had consistently low expression values, while the other mouse had consistently high expression values. TLL082 was likely working in the mouse expressing lower levels of the inflammatory markers at a dose of 10 mg/kg.

When we dissolved TLL082 in the PEG300:ddH₂O vehicle we found that at both doses the mixture looked cloudy, although uniformly distributed. The precipitate settled in the bottle when left alone but got uniformly redistributed when manually shaken. We made sure to shake the mixtures when dosing the mice. TLL041 on the other hand looked completely clear at both doses, although sometimes particles could be seen at the 10 mg/kg dose. We were told that the two compounds are slightly different in structure, which likely affects the polarity of TLL082 making it more difficult to dissolve. We suspect that poor dissolution of the compounds may have affected our results. Some of the mice may have not been able to properly digest the compounds so they could have their full effect. In the future, we plan to test new vehicles that can properly dissolve TLL082 to produce a clear mixture like with TLL041 at 3.3 mg/kg.

Another possible issue with drug dissolution was the use of the sonicator. If allowed to sonicate for too long, the compounds are at risk of getting oxidized. When making the drugs, we sometimes got foamy solutions after sonicating, which could be an indication that the compounds were oxidized. In the future, we may try to dissolve our drugs by using a different method of mixing such as a pestle to avoid the possibility of oxidation.

CONCLUSION

TLL041 and TLL082 are dual TYK2/JAK1 kinase inhibitors developed to suppress signaling in the type I interferon pathway, which can be stimulated by cdsRNA in neurodegenerative diseases.

TLL041 reduced all inflammatory marker gene expression tested at a dose of 3.3 mg/kg that was statistically significant. The effects of TLL041 at 10 mg/kg and TLL082 at 3.3 mg/kg and 10 mg/kg were not statistically significant, but there were some responders that brought down inflammation in some, but not all Nd1 mice. It is possible that lack of statistical significance is due to incomplete dissolution of the compounds in the vehicle used in this study. PK results which will be obtained later may help corroborate this notion.

Rodriguez et al have previously reported that JAK inhibitors such as ruxolitinib and baricitinib were able to bring down neuroinflammation in Nd1 mice by targeting the JAK1 kinase on the type I interferon receptor. However, these drugs are not as specific to the type I interferon receptor as the TLL compounds are, and may therefore have off-target effects. The fact that the TLL compounds target only JAK1 and TYK2 kinases makes these drugs less likely to have off-

target effects. Therefore, the TLL compounds might be a safer treatment option for neurodegenerative disease patients.

The results are preliminary, and there will be further testing of both compounds in Nd1 mice in the near future. We plan to run a qPCR analysis for all treatment groups to test for the expression levels of some other inflammatory markers, and markers of neuronal death to see if there was any neuronal rescue. An IHC antibody staining of these samples will also provide further evidence on whether or not these drugs are effective, and if blocking TYK2/JAK1 kinase activity in the type I interferon signaling cascade is an effective treatment method for neurodegenerative diseases.

REFERENCES

- Barrat, Franck J et al. "Importance of Nucleic Acid Recognition in Inflammation and Autoimmunity." *Annual review of medicine* vol. 67 (2016): 323-36. doi:10.1146/annurev-med-052814-023338
- Chang, Rudy et al. "Tumor necrosis factor α Inhibition for Alzheimer's Disease." *Journal of central nervous system disease* vol. 9 1179573517709278. 15 May. 2017, doi:10.1177/1179573517709278
- Chen, Shih-Yuan et al. "Sequence variants of interleukin 6 (IL-6) are significantly associated with a decreased risk of late-onset Alzheimer's disease." *Journal of neuroinflammation* vol. 9 21. 24 Jan. 2012, doi:10.1186/1742-2094-9-21
- Decourt, Boris et al. "Targeting Tumor Necrosis Factor Alpha for Alzheimer's Disease." *Current Alzheimer research* vol. 14,4 (2017): 412-425. doi:10.2174/1567205013666160930110551
- Dileep, Vishnu et al. "Neuronal DNA double-strand breaks lead to genome structural variations and 3D genome disruption in neurodegeneration." *Cell* vol. 186,20 (2023): 4404-4421.e20. doi:10.1016/j.cell.2023.08.038
- Domingo-Prim, Judit et al. "RNA at DNA Double-Strand Breaks: The Challenge of Dealing with DNA:RNA Hybrids." *BioEssays : news and reviews in molecular, cellular and developmental biology* vol. 42,5 (2020): e1900225. doi:10.1002/bies.201900225
- Field, Robert et al. "Systemic challenge with the TLR3 agonist poly I:C induces amplified IFN α /beta and IL-1beta responses in the diseased brain and exacerbates chronic neurodegeneration." *Brain, behavior, and immunity* vol. 24,6 (2010): 996-1007. doi:10.1016/j.bbi.2010.04.004
- Fu, Jiajia et al. "The role of Th17 cells/IL-17A in AD, PD, ALS and the strategic therapy targeting on IL-17A." *Journal of neuroinflammation* vol. 19,1 98. 22 Apr. 2022, doi:10.1186/s12974-022-02446-6
- Huys, Liesbeth et al. "Type I interferon drives tumor necrosis factor-induced lethal shock." *The Journal of experimental medicine* vol. 206,9 (2009): 1873-82. doi:10.1084/jem.20090213

- Kim, Young Hye et al. "A 3D human neural cell culture system for modeling Alzheimer's disease." *Nature protocols* vol. 10,7 (2015): 985-1006. doi:10.1038/nprot.2015.065
- Klein, Julia et al. "Olfactory Impairment Is Related to Tau Pathology and Neuroinflammation in Alzheimer's Disease." *Journal of Alzheimer's disease : JAD* vol. 80,3 (2021): 1051-1065. doi:10.3233/JAD-201149
- LaRocca, Thomas J et al. "TDP-43 knockdown causes innate immune activation via protein kinase R in astrocytes." *Neurobiology of disease* vol. 132 (2019): 104514. doi:10.1016/j.nbd.2019.104514
- Liang, C., Xixi, D., Tang W., Wanke Q., *Methods of Treating CNS Disorders*. WO 2023/035913 A1, 22.08.2022, 16.03.2023
- McClintock, Timothy S et al. "Maturation of the Olfactory Sensory Neuron and Its Cilia." *Chemical senses* vol. 45,9 (2020): 805-822. doi:10.1093/chemse/bjaa070
- Murira, Armstrong, and Alain Lamarre. "Type-I Interferon Responses: From Friend to Foe in the Battle against Chronic Viral Infection." *Frontiers in immunology* vol. 7 609. 19 Dec. 2016, doi:10.3389/fimmu.2016.00609
- Murray, Carol et al. "Interdependent and independent roles of type I interferons and IL-6 in innate immune, neuroinflammatory and sickness behaviour responses to systemic poly I:C." *Brain, behavior, and immunity* vol. 48 (2015): 274-86. doi:10.1016/j.bbi.2015.04.009
- Nature News and Views: Chromosomes come together to help mice distinguish odours | COLUMBIA | Lomvardas Lab. (n.d.). Retrieved March 7, 2024, from <https://lomvardaslab.zuckermaninstitute.columbia.edu/news/nature-news-and-views-chromosomes-come-together-help-mice-distinguish-odours>
- Ochoa, Elizabeth et al. "Pathogenic tau-induced transposable element-derived dsRNA drives neuroinflammation." *Science advances* vol. 9,1 (2023): eabq5423. doi:10.1126/sciadv.abq5423
- Platanias, Leonidas C. "Mechanisms of type-I- and type-II-interferon-mediated signaling." *Nature reviews. Immunology* vol. 5,5 (2005): 375-86. doi:10.1038/nri1604

- Purves, D. et al. "Odorant Receptors and Olfactory Coding." Neuroscience, 2nd edition (2001), Sinauer Associates.
<https://www.ncbi.nlm.nih.gov/books/NBK10824/>
- Rahman, M Mahafuzur, and Christofer Lendel. "Extracellular protein components of amyloid plaques and their roles in Alzheimer's disease pathology." Molecular neurodegeneration vol. 16,1 59. 28 Aug. 2021, doi:10.1186/s13024-021-00465-0
- Rodriguez, Steven et al. "Innate immune signaling in the olfactory epithelium reduces odorant receptor levels: Modeling transient smell loss in COVID-19 patients." *medRxiv*, 2020.06.14.20131128.
<https://doi.org/10.1101/2020.06.14.20131128>
- Rodriguez, Steven et al. "Genome-encoded cytoplasmic double-stranded RNAs, found in C9ORF72 ALS-FTD brain, propagate neuronal loss." Science translational medicine vol. 13,601 (2021): eaaz4699. doi:10.1126/scitranslmed.aaz4699
- Vellecco, Valentina et al. "Interleukin-17 (IL-17) triggers systemic inflammation, peripheral vascular dysfunction, and related prothrombotic state in a mouse model of Alzheimer's disease." Pharmacological research vol. 187 (2023): 106595. doi:10.1016/j.phrs.2022.106595
- Zhang, Weifeng et al. "Role of neuroinflammation in neurodegeneration development." Signal transduction and targeted therapy vol. 8,1 267. 12 Jul. 2023, doi:10.1038/s41392-023-01486-5